ELSEVIER

Earth and Planetary Science Letters 160 (1998) 563–568

EPSL

Transitions in the style of mantle convection at high Rayleigh numbers

Dayanthie Weeraratne, Michael Manga *

Department of Geological Sciences, University of Oregon, Eugene, OR 97403, USA

Received 9 February 1998; revised version received 1 May 1998; accepted 11 May 1998

Abstract

The pattern and style of mantle convection govern the thermal evolution, internal dynamics, and large-scale surface deformation of the terrestrial planets. In order to characterize the nature of heat transport and convective behaviour at Rayleigh numbers, Ra, appropriate for planetary mantles (between 10^4 and 10^8), we perform a set of laboratory experiments. Convection is driven by a temperature gradient imposed between two rigid surfaces, and there is no internal heating. As the Rayleigh number is increased, two transitions in convective behaviour occur. First we observe a change from steady to time-dependent convection at $\mathrm{Ra} \approx 10^5$. A second transition occurs at higher Rayleigh numbers, $\mathrm{Ra} \approx 5 \times 10^6$, with large-scale time-dependent flow being replaced by isolated rising and sinking plumes. Corresponding to the latter transition, the exponent β in the power law relating the Nusselt number Nu to the Rayleigh number ($\mathrm{Nu} \sim \mathrm{Ra}^{\beta}$) is reduced. Both rising and sinking plumes always consist of plume heads followed by tails. There is no characteristic frequency for the formation of plumes.

Keywords: mantle; convection; thermal history; plumes

1. Introduction

Both the vigour and pattern of mantle convection change over time. In the Earth's mantle, the time-dependence of convective motions can be related to the formation of mantle plumes and changes in plate motion and geometry. Time-dependence is reflected in hotspot activity [1], continent aggregation and breakup on the Earth, and the possible global resurfacing on Venus [2]. On time scales of billions of years, changes in convective behaviour may accompany the secular cooling of planets [3,4].

In order to study time-dependent convective behaviour and heat transport at Rayleigh numbers relevant for planetary mantles, we perform a set of nineteen laboratory experiments. We adopt an experimental approach because it allows us to study high Rayleigh number convection in three dimensions with fluids that have a temperature-dependent viscosity [5], though we are unable to simulate important aspects of convection in the Earth's mantle such as plates and internal heating.

2. Experimental approach

Our model mantle consists of a tank of Newtonian corn syrup with glass side walls and an aluminum top and bottom. The temperatures at the top and bottom of the tank, T_0 and T_1, respectively, are controlled by circulating water. The entire apparatus

* Corresponding author. Tel.: +1 (541) 346-5574; Fax: +1 (541) 346-4692; E-mail: manga@newberry.uoregon.edu

0012-821X/98/$19.00
PII S0012-821X(98)00111-3

is insulated with 5-cm-thick polystyrene foam. Two sets of experiments are performed. The first set uses a tank with aspect ratio 3 : 1 (30 × 30 × 10 cm) and is intended to reproduce previous low Rayleigh number experimental results and test our methodology. The second set uses a tank with aspect ratio 1 : 1 (33 × 33 × 33 cm). The greater depth allows us to achieve Rayleigh numbers two orders of magnitude higher than previous equilibrium results [6–9], but at the expense of a large aspect ratio. However, we find that at such high Rayleigh numbers, heat transport is dominated by plumes that are small compared to the tank width so that the effect of the small aspect ratio is reduced.

Temperatures T_1, T_0, and within the tank are measured by an array of 27 J-type thermocouples at time intervals of 1 to 15 s. Six probes, hereafter referred to as the 'middle thermocouples', are located halfway between the top and bottom of the tank and at various horizontal positions. Ten thermocouples are located 3.0 mm below the upper surface in order to measure the surface heat flux, and are distributed over the surface. Heat transport is characterized by the Nusselt number, Nu, which is the ratio of the total surface heat flux to that conducted in the absence of convection. Thermal equilibrium is determined by ensuring that both the mean Nu and internal temperature are constant [10]. All results are based on equilibrium conditions, and we analyze time series with lengths ranging from 2 days to 8 h for the lowest and highest Rayleigh numbers, respectively. The convective behaviour of a fluid heated from below and cooled from above is determined by the Rayleigh number

$$\mathrm{Ra}_{1/2} = \frac{\rho g \alpha (T_1 - T_0) d^3}{\mu_{1/2}\kappa} \tag{1}$$

where the subscript 1/2 denotes material properties evaluated at the median temperature, $(T_1 + T_0)/2$. Previous experimental studies of convection between rigid surfaces have shown that Nu depends only on $\mathrm{Ra}_{1/2}$ and not on the magnitude of viscosity variations [6,7,9]. Here, ρ, g, α, κ, μ and d are the density, gravitational acceleration, thermal expansivity, thermal diffusivity, viscosity and tank depth, respectively. Values for these properties are listed in Tables 1 and 2. We assume an uncertainty of 20% for $\mathrm{Ra}_{1/2}$, due primarily to uncertainties of κ and α. At the highest $\mathrm{Ra}_{1/2}$ we achieve, 1.2×10^8, the Reynolds number $\mathrm{Re} = \rho u L/\mu$ is less than 0.5; this upper bound is based on $\mu(T_1)$, and the measured plume head radius and rise speed of $L = 2$ cm and $u = 3$ mm/s, respectively. Inertial effects can thus be neglected for all our experiments because even for Re ~ 1 the velocity of buoyant regions is largely unaffected by inertia [11].

Table 1
Material properties

Property	Symbol	Value or range
Density [a]	ρ	1.390 to 1.431 g/cm^3
Thermal expansivity [b]	α	4.0×10^{-4}°C^{-1}
Thermal diffusivity [b]	κ	1.1×10^{-7} m^2/s
Viscosity [c]	$\mu_{1/2}$	0.76 to 181 Pa s
Temperature difference	$T_1 - T_0$	19.5 to 68.5°C
Tank depth	d	10 or 33 cm

[a] Measured with a glass hydrometer. [b] From Giannandrea and Christensen [9]. [c] Measured with rotational viscometer; $\mu_{1/2} = \mu(T_{1/2})$, where $T_{1/2} = (T_1 + T_0)/2$. See Refs. [5,7–9] for the form of the temperature-dependence.

Table 2
Dimensionless parameters

Parameter	Definition	Range
Rayleigh number	$\mathrm{Ra}_{1/2} = \frac{\rho g \alpha (T_1 - T_0) d^3}{\mu_{1/2}\kappa}$	8.6×10^3 to 1.2×10^8
Prandtl number	$\mathrm{Pr} = \mu_{1/2}/\rho\kappa$	4.9×10^3 to 1.1×10^6
Viscosity ratio	$\mu(T_0)/\mu(T_1)$	6.39 to 397
Reynolds number [a]	$\mathrm{Re} = \rho u L/\mu$	<0.5

[a] Here u and L are the velocity and length scale characteristic of fluid motions; the upper bound is for the experiment at the highest $\mathrm{Ra}_{1/2}$.

3. Results and discussion

We determine time-dependent convective style from temperatures recorded by the middle thermocouples. At $\mathrm{Ra}_{1/2}$ less than about 10^5, flow is steady and temperatures remain constant. As $\mathrm{Ra}_{1/2}$ is increased, e.g. Fig. 1a for $\mathrm{Ra}_{1/2} = 2.7 \times 10^5$, flow becomes unsteady and temperature fluctuations have a large amplitude and a long period. As $\mathrm{Ra}_{1/2}$ is increased still further, e.g. Fig. 1b for $\mathrm{Ra}_{1/2} = 4.7 \times 10^6$, the amplitude of long-period temperature fluctuations decreases. At still higher $\mathrm{Ra}_{1/2}$,

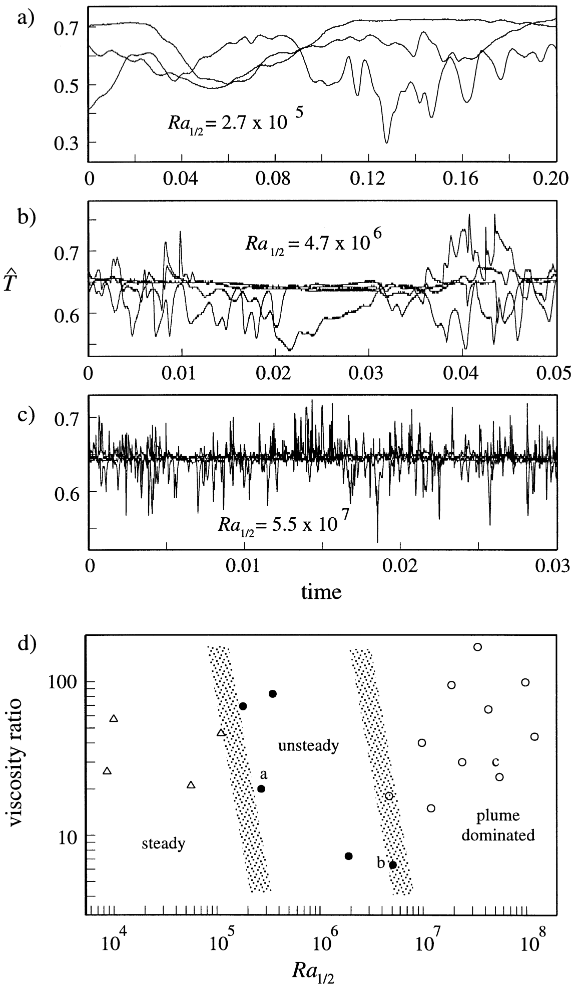

Fig. 1. Temperature fluctuations at three or four middle thermocouples under conditions of thermal equilibrium. (a) Unsteady convection dominated by large scale flow ($\mathrm{Ra}_{1/2} = 2.7 \times 10^5$). (b) Increased plume activity along with large-scale flow ($\mathrm{Ra}_{1/2} = 4.7 \times 10^6$). (c) Plume-dominated convection with short period fluctuations and a constant average temperature ($\mathrm{Ra}_{1/2} = 5.5 \times 10^7$). Dimensionless temperature, $\hat{T}$, is defined as $(T - T_0)/(T_1 - T_0)$. Time is normalized by the diffusive time d^2/κ. (d) Summary of experimental results. The viscosity ratio is $\mu(T_0)/\mu(T_1)$. Shaded area shows the estimated transitions between the three styles of convection: steady, unsteady, and plume-dominated flow. The transition to plume-dominated flow is gradual. The letters *a–c* indicate the experiments shown in (a)–(c).

the middle thermocouples have a constant average temperature and show no evidence for large-scale flow, e.g. Fig. 1c for $\mathrm{Ra}_{1/2} = 5.5 \times 10^7$. We attribute the short-period temperature fluctuations in Fig. 1 to rising and sinking thermal plumes. We refer to flows in which we only observed short-period temperature fluctuations, e.g. Fig. 1c, as 'plume-dominated' convection. Indeed, in this limit we observe rising and sinking mushroom-shaped plumes, as shown in Fig. 2. These plumes always appear to consist of a plume head and tail. The detached plume heads observed by Yuen et al. [12] in 2D numerical calculations with free-slip boundaries may be due to the presence of a large-scale flow [13] and do not occur in 3D calculations [14]. In Fig. 1d, we summarize the conditions at which we observe each of the three convective styles: steady, unsteady, and plume-dominated.

In Fig. 3a, we show histograms of the temperature fluctuations corresponding to Fig. 1a–c. For the flows that we call 'unsteady', see Fig. 1d, we observe a broad distribution with a superimposed peak at $\hat{T} \approx 0.7$ that is due to coexisting plumes. Here, $\hat{T} = (T - T_0)/(T_1 - T_0)$ is a normalized temperature. For plume-dominated flows, we observe a narrow distribution that is approximately exponential. Experimental studies with low Prandtl number fluids (very high Reynolds numbers), find an abrupt change in the distribution of temperature fluctuations, from a Gaussian to an exponential distribution, that defines the transition to 'hard thermal turbulence' [15,16]. Our distributions change gradually with increasing

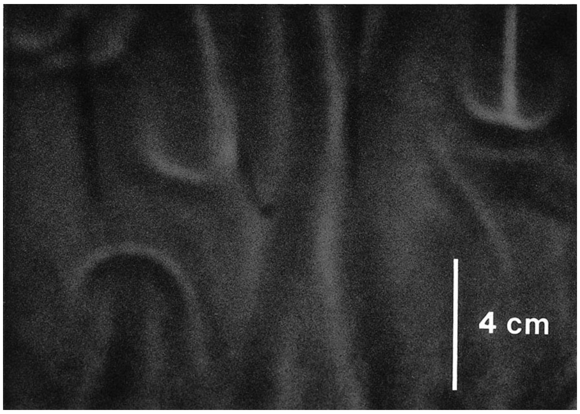

Fig. 2. Shadowgraph showing rising and sinking mushroom-shaped plumes with tails for $\mathrm{Ra}_{1/2} = 5.5 \times 10^7$. The shadows cast by three thermocouples are visible in the upper left of the figure. Shadowgraphs are made by temporarily removing pieces of insulation from the sides of the tank.

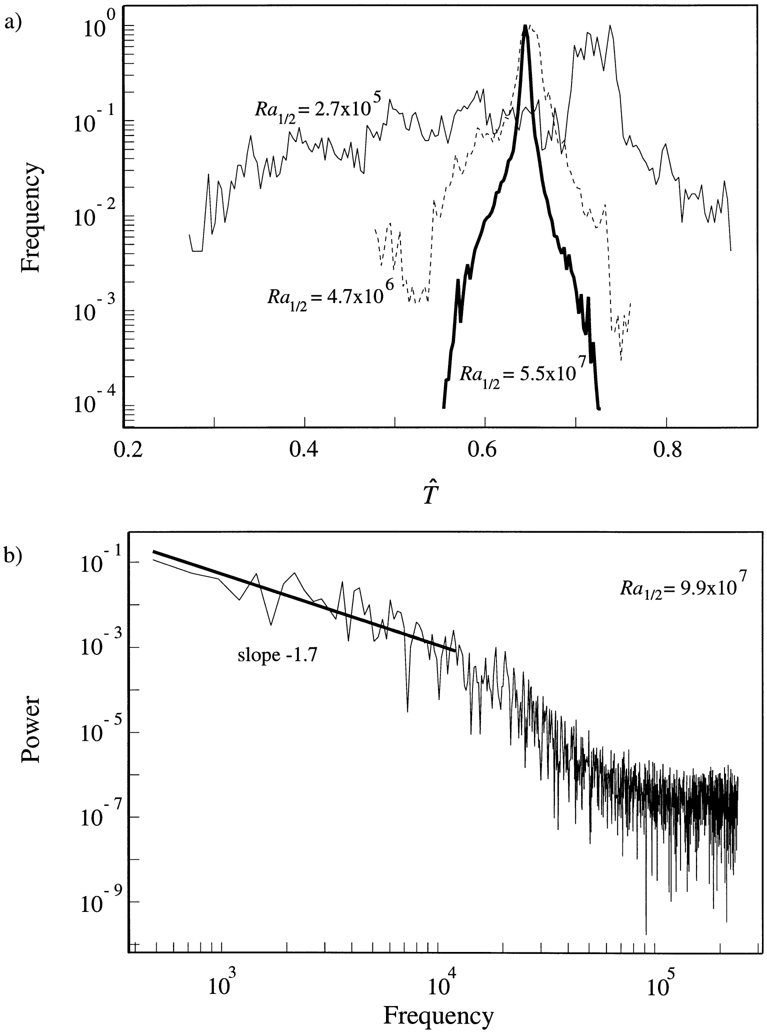

Fig. 3. (a) Distribution of temperature fluctuations at all of the middle thermocouples for the experiments shown in Fig. 1a–c. Temperature is normalized as in Fig. 1. (b) Power spectrum of temperature fluctuations for $Ra_{1/2} = 9.9 \times 10^7$; frequency is normalized by the diffusive time scale.

Ra, reflecting a gradual change in the relative importance of large-scale flows and plumes.

Previous studies have used power spectra to clarify transitions in time-dependent convection [17]. Similar to the gradual changes in the histograms in Fig. 3a, the slope of the power spectra at low frequencies also increases gradually as Ra is increased. In Fig. 3b we show the power spectrum of temperature fluctuations at the middle thermocouples for $Ra_{1/2} = 9.9 \times 10^7$. The higher Ra is chosen for comparison with numerical calculations: we find a slope of -1.7 similar to the slope obtained by Yuen et al. [12] for the Nu power spectrum. For all experiments, we observe no dominant frequency at the middle thermocouples, in contrast to the experiments performed at low Prandtl numbers [15,16].

In Fig. 4 we plot Nu against $Ra_{1/2}$. Our measurements for $Ra_{1/2}$ up to $\approx 10^6$ are consistent with previous results [6,7,9] which find a slope of ≈ 0.28. For $Ra_{1/2}$ greater than 5×10^6 we observe a distinct (and continual) decrease in slope corresponding to the transition to plume-dominated convection, with

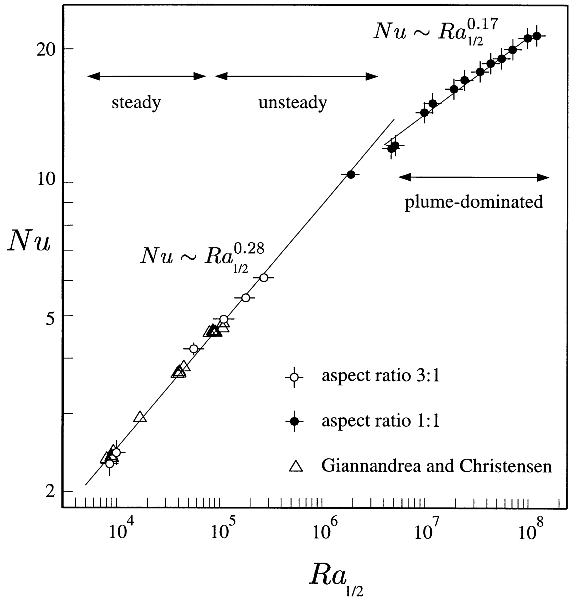

Fig. 4. Nusselt number as a function of $Ra_{1/2}$. Results for $Ra_{1/2}$ less than 10^6 agree with previous studies [9]. Uncertainty in $Ra_{1/2}$ is based on an estimated uncertainty in κ and α. Uncertainties for Nu at $Ra_{1/2} > 10^6$ are standard deviations of temporal fluctuations of Nu; uncertainties at lower $Ra_{1/2}$ are based on the measurement accuracy of the thermocouples of 0.1 degrees.

$Nu \sim Ra_{1/2}^{0.17}$. This exponent is about half the classical value of 1/3 [18,19] employed in parametrized thermal evolution models [20–22]. Interestingly, this exponent is nearly identical to that found in secular heating experiments at similar Ra by Lithgow-Bertelloni et al. [23]. Three-dimensional numerical calculations, however, do not find a similar break in slope ([14], P. Tackley, pers. commun.). It is possible that our thermocouple probes (diameter of the glass thermocouple casing is 1.3 mm) influence the flow and Nu. In particular, if the probes establish preferred sites of downwelling, then Nu will be underestimated. We also note that, due to the finite thickness (6.5 mm) and thermal conductivity of the aluminum plates on the top and bottom of the tank, our boundary conditions are not isothermal, and will be affected by the flow.

Although our experimental model does not account for all important features of the Earth's mantle, in particular internal heating and mobile surface plates, our results illustrate fundamental convective processes that occur at Earth-like Rayleigh numbers. Specifically, we find a large reduction in the rate of convective heat transport at very high Ra which implies significantly less secular cooling over Earth's history [24].

Finally, our no-slip boundary may be appropriate for one-plate planets such as Venus. Analyses of the geoid and surface deformation suggest that large-scale convection occurs within the Venusian mantle [25]. In order for such large-scale convection to exist beneath a rigid surface, our experimental results indicate that $Ra_{1/2}$ must be less than about 5×10^6, that is, convection is unsteady and not plume-dominated. However, at such low Ra, thermal plumes will be too large and will form too infrequently to create coronae. Coronae are surface features observed on Venus that are thought to be formed by diapirs or plume heads with diameters of $\sim$100 km [26,27]. Coronae forming diapirs must thus form by some mechanism other than thermal boundary layer instabilities.

Acknowledgements

This work was supported by NSF through a CAREER grant and REU supplements. D. Senkovich and K. Johnson provided technical assistance. We thank L. Magde, B. Hager, C. Lithgow-Bertelloni and P. Tackley for comments. ***[RO]***

References

[1] M.A. Richards, R.A. Duncan, V.E. Courtillot, Flood basalts and hotspot tracks: plume heads and tails, Science 246 (1989) 103–107.
[2] R.R. Herrick, Resurfacing history of Venus, Geology 22 (1994) 703–706.
[3] U. Hansen, D.A. Yuen, High Rayleigh number regime of temperature-dependent viscosity convection and the Earth's early thermal history, Geophys. Res. Lett. 20 (1993) 2191–2194.
[4] V. Steinbach, D.A. Yuen, Zhao, Instabilities from phase transitions and the timescales of mantle thermal evolution, Geophys. Res. Lett. 20 (1993) 1119–1122.
[5] A. Davaille, C. Jaupart, Transient high-Rayleigh-number thermal convection with large viscosity variations, J. Fluid Mech. 253 (1933) 141–166.
[6] J.R. Booker, Thermal convection with strongly temperature-dependent viscosity, J. Fluid Mech. 76 (1976) 741–754.

[7] F.M. Richter, H. Nataf, S.F. Daly, Heat transfer and horizontally averaged temperature of convection with large viscosity variations, J. Fluid Mech. 129 (1983) 173–192.
[8] D.B. White, The planforms and onset of convection with a temperature-dependent viscosity, J. Fluid Mech. 191 (1988) 247–286.
[9] E. Giannandrea, U. Christensen, Variable viscosity convection experiments with a stress-free upper boundary and implications for the heat transport in the Earth's mantle, Phys. Earth Planet. Inter. 78 (1993) 139–152.
[10] B. Travis, P. Olson, Convection with internal heat sources and thermal turbulence in the Earth's mantle, Geophys. J. Int. 118 (1994) 1–19.
[11] G.K. Batchelor, An Introduction to Fluid Dynamics, Cambridge University Press, Cambridge, 1967, 615 pp.
[12] D.A. Yuen, W. Zhao, A.P. Vincent, A.V. Malevsky, Hard turbulent thermal convection and thermal evolution of the mantle, J. Geophys. Res. 98 (1993) 5355–5373.
[13] U. Hansen, D.A. Yuen, S.E. Kroening, Transition to hard turbulence in thermal convection at infinite Prandtl number, Phys. Fluids A 2 (1990) 2157–2163.
[14] R.A. Trompert, U. Hansen, On the Rayleigh number dependence of convection with a strongly temperature-dependent viscosity, Phys. Fluids 10 (1998) 351–360.
[15] F. Heslot, B. Castaing, A. Libchaber, Transitions to turbulence in helium gas, Phys. Rev. A 36 (1987) 5870–5873.
[16] B. Castaing, G. Gunaratne, F. Heslot, L. Kadanoff, A. Libchaber, S. Thomae, X.Z. Wu, S. Zaleski, G. Zanetti, Scaling of hard thermal turbulence in Rayleigh–Benard convection, J. Fluid Mech. 204 (1989) 1–30.
[17] X.Z. Wu, L. Kadanoff, A. Libchaber, M. Sano, Frequency power spectrum of temperature fluctuations in free convection, Phys. Rev. Lett. 64 (1990) 2140–2143.
[18] D.L. Turcotte, E.R. Oxburgh, Finite amplitude convective cells and continental drift, J. Fluid Mech. 28 (1967) 29–42.
[19] V.S. Solomatov, Scaling of temperature- and stress-dependent viscosity convection, Phys. Fluids 7 (1995) 266–274.
[20] H.N. Sharpe, W.R. Peltier, Parameterized convection and the Earth's thermal history, Geophys. Res. Lett. 5 (1978) 737–740.
[21] G. Schubert, P. Cassen, R.E. Young, Core cooling by subsolidus mantle convection, Phys. Earth Planet. Inter. 20 (1979) 194–209.
[22] G.F. Davies, Thermal histories of convective earth models and constraints on radiogenic heat production in the Earth, J. Geophys. Res. 285 (1980) 2517–2530.
[23] C. Lithgow-Bertelloni, M.A. Richards, R.W. Griffiths, C. Conrad, Plume generation in natural convection at high Rayleigh and Prandtl numbers, J. Fluid Mech. (1998) submitted.
[24] S. Morris, D. Canright, A boundary-layer analysis of Benard convection in a fluid of strongly temperature-dependent viscosity, Phys. Earth Planet. Inter. 36 (1984) 355–373.
[25] M. Simons, B.H. Hager, S.C. Solomon, Global variations in the geoid/topography admittance of Venus, Science 264 (1994) 798–803.
[26] E.R. Stofan, D.L. Bindschadler, J.W. Head, E.M. Parmentier, Corona structures on Venus: models of origin, J. Geophys. Res. 96 (1991) 20933–20946.
[27] D.M. Koch, M. Manga, Neutrally buoyant diapirs — a model for Venus coronae, Geophys. Res. Lett. 23 (1996) 225–228.